NSF 1530603: SNM: Low-Cost, Large-Scale Nanomanufacturing of Superinsulating Aerogels & Lightweight, Mechanically-Strong Aerogels

Marc Hodes, Nicholas Leventis and Stephen Steiner

Tufts University, Missouri University of Science & Technology and Aerogel Technologies

Introduction

Key bottlenecks stifling cost- and energy-efficient continuous nanomanufacturing of existing and emerging aerogel materials are investigated to directly and deterministically design low-cost, rapid, scalable drying processes. We measure the density of and diffusion coefficient in supercritical CO_2-solute mixtures. We also study the role of fluid-composition-dependent compressibility effects and their influence on transport and drying phenomena and mechanical strain during supercritical drying of target materials. We also study the origin of drying shrinkage of silica aerogels and explore alternative methods to prevent it, minimize it, or at least control it.

Transport Model

- The geometry considered is an inner annulus of silica aerogel, concentric with an outer annulus through which supercritical carbon dioxide ($SCCO_2$) is pumped, as shown in Fig. 1. As the fluid inside the pore changes from pure ethanol to pure CO_2, its density changes non-monotonically. This causes a non-zero velocity at the porous region-free flow interface that has been referred to in the literature as a suction/spillage effect, which is quantified here by modeling convective mass transfer. The aerogel is modeled as a porous medium using Darcy's Law and the outer annulus as an open region (free flow). Compressibility effects are captured in the coupled regions as is a mass fraction-dependent molecular diffusivity in the species equations.

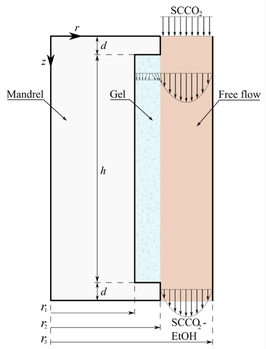

Fig. 1: 2D axisymmetric model.

- Mass, momentum, species transport equations in free flow:

Mass: $$\frac{\partial \rho}{\partial t} + \nabla \cdot (\rho \boldsymbol{u}) = 0$$

Momentum: $$\rho \frac{\partial \boldsymbol{u}}{\partial t} + \rho (\boldsymbol{u} \cdot \nabla \boldsymbol{u}) = -\nabla p + \mu \nabla^2 \boldsymbol{u} + \frac{1}{3} \mu \nabla (\nabla \cdot \boldsymbol{u})$$

Species: $$\frac{\partial}{\partial t}(\rho m_E) + \nabla \cdot (\rho m_E \boldsymbol{u}) = \nabla \cdot \left[D_{ij} \nabla (\rho m_E) \right]$$

Properties: $$p = p(m_E, \rho, t) \;\&\; D_{ij} = D_{ij}(m_E, \rho, t)$$

- Volume averaged governing equations in the porous media (gel):

Mass: $$\frac{\partial \langle \varepsilon \rho \rangle}{\partial t} + \nabla \cdot \langle \rho \boldsymbol{u} \rangle = 0$$

Momentum: $$\frac{\mu}{\boldsymbol{K}} \langle \boldsymbol{u} \rangle = -\nabla \langle p \rangle$$

Species: $$\frac{\partial}{\partial t} \langle \rho m_E \rangle + \nabla \cdot \langle \rho m_E \boldsymbol{u} \rangle = \nabla \cdot \langle D_{ij} \nabla (\rho m_E) \rangle$$

Properties: $$p = p(m_E, \rho, t) \;\&\; D_{ij} = D_{ij}(m_E, \rho, t)$$

- Model parameters:

Parameters	Symbol		Unit
Inlet velocity	w_{in}	0.605×10^{-3}	m/s
Outlet pressure	p_{ref}	12.4	MPa
Porosity	ε	0.9	–
Permeability	$\boldsymbol{K}$	10^{-12}	m^2
Viscosity	μ	4.61×10^{-5}	Pa · s
Mandrel top	d	5	mm
Alcogel height	h	220	mm
Alcogel inner radius	r_1	25.5	mm
Alcogel outer radius	r_2	28	mm
Vessel inner radius	r_3	38.1	mm

Numerical Results

- Initially, as CO_2 diffuses into the ethanol-rich pores, the fluid mixture becomes denser than pure ethanol, creating suction along the gel-free flow interface.
- As drying progresses, the fluid density decreases at lower mass fractions of ethanol. Thus, the fluid mixture in pores gains in volume and spills across the gel-free interface into the $SCCO_2$ free flow per Fig. 2. At the top of the gel, suction occurs at locations closer to the aluminum mandrel and spillage closer to the gel-free interface.

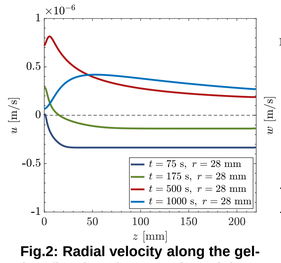

Fig.2: Radial velocity along the gel-free flow interface at selected times.

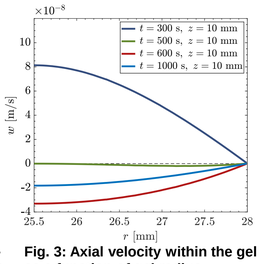

Fig. 3: Axial velocity within the gel as a function of gel radius.

- Suction and spillage impose changes in the axial velocity initially generated from the shear stress exerted by the $SCCO_2$ free flow at the gel-free flow interface
- The axial velocity changes magnitude and direction not only over time, but also with distance from the inlet to account for the shrinkage and expansion of the fluid in the pores per Fig. 3.

Density Rig

- The density rig, as shown in Fig. 4, measures density and viscosity of alcohol-CO_2 solutions as $f(T, p,$ solute concentration) at supercritical conditions with high speed and accuracy.

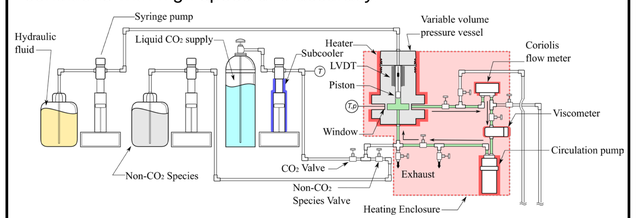

Fig. 4: Schematic of density rig.

- Adjustable measurement parameters:
  - Mass flow rate (via circulation pump up to 25 kg/hr).
  - Volume of test section is 45 – 52 mL.
  - Pressure: Mixture critical pressure (e.g., 1300 psi at 323K) to 2500 psi (max pressure of Coriolis flow meter).
  - Temperature: 313K to 348K. (up to 75°C)
  - CO_2 and solvent mass fraction.

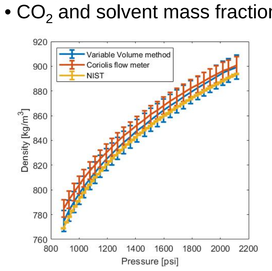

Fig. 5: Density of pure CO_2 at 21.25°C.

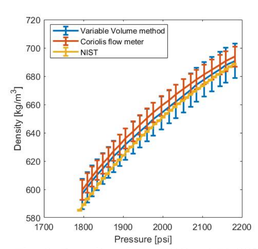

Fig. 6: Density of pure CO_2 at 51.33°C.

- Fig. 5 and Fig. 6 show the pure CO_2 density measurements from the variable volume method and Coriolis flow meter compared to NIST Chemistry WebBook.

Sorét Diffusion Coefficient Rig

- Design, construct, commission and utilize new rig to measure Fick and Sorét diffusion coefficients of alcohol-CO_2 solutions as $f(T, p,$ solute concentration) at supercritical conditions.
- Using laser-induced grating method, these parameters will be measured in a non-invasive and contact-free manner.

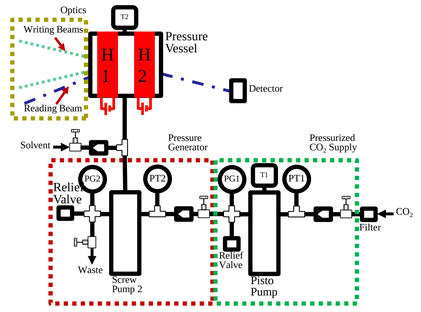

Fig. 7: Schematic of the Sorét diffusion coefficient rig.

Why Aerogels Shrink During SCF Drying?

- The origin of drying shrinkage was investigated by employing silica wet-gels formed via base-catalyzed hydrolysis and polycondensation of tetramethylorthosilicate (TMOS).
- In order to deconvolute drying shrinkage from syneresis, wet-gels were processed into aerogels at seven different stages during aging (2, 4, 8, 12, 16, 20 and 24 h) (Figure 8). The pore-filling gelation solvent in the 24 h aged wet-gels were exchanged with non H-bonding toluene and xylene and shrinkage was measured during processing (Figure 9).

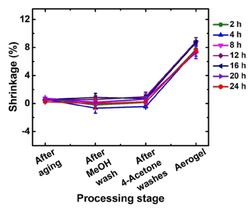

Fig. 8: Shrinkage for all Gels with Aging Time and Processing Stage

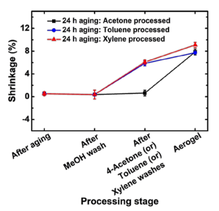

Fig. 9: Shrinkage of Aerogels vs Wet-gels in Different Solvents

- Wet silica gels are stabilized by polar/H-bonding interactions between surface Si-OH groups and the pore solvent (acetone). That interaction is lost in wet-gels with non-H-bonding solvents and in aerogels.
- In those cases, to maintain H-bonding, particles come closer and interactions between surface Si-OH groups are maximized (Scheme 1).

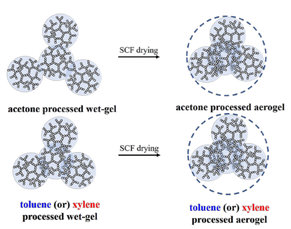

Scheme 1: Proposed mechanism for shrinkage during drying

- Table 1 shows that all samples are mass fractals, therefore they have plenty of internal empty space to accommodate the smaller primary particles of a neighboring assembly, as the two assemblies come closer.

Table 1: Fractal dimension of aerogels using SAXS

Sample	Fractal dimension SAXS
24h Acetone	2.36 ± 0.23
24h Toluene	2.79 ± 0.33
24h Xylene	2.33 ± 0.49

Optics Rig

- $NaYF_4$:Yb/Er upconverting nanoparticles embedded in transparent silica aerogel monoliths at concentration 0.01 mg/mL will fluoresce in the visible range (540 nm green light emission) when exposed to 500 mW of IR laser light (980 nm). Voxel size and aspect ratio are decreased to roughly 1 mm diameter and roughly 1:1 via an aspheric focusing lens and rapid mechanical pulsing of the laser (effective duty cycle of 1%, 50 µs "on" and 4950 µs "off") (Fig. 10). Optical interrogation of the volume of the monolith is achieved via linear stages controlled by stepper motors; the laser focal point is held stationary while the monolith is moved through 3D space, allowing for fluorescence to be induced throughout the volume of the monolith (Fig. 11).

Fig. 10: Voxel size (~1 mm diameter) and aspect ratio (~1:1) after pulsing at 1% duty cycle

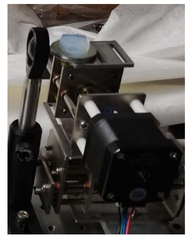

Fig. 11: Optical interrogation throughout volume of monolith via linear stages

- Initial experiments observing the relationship between applied strain and induced fluorescence intensity demonstrate a different result than was hypothesized: as strain increases, the fluorescence intensity seems to decrease on average (Fig. 12). However, the relationship is heavily dependent on the location of the voxel, suggesting high heterogeneities in nanoparticle distribution.

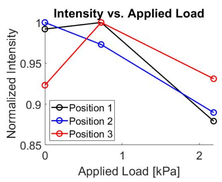

Fig. 12: Fluorescence and applied load as a function of spatial position

- In addition, the fluorescence is also heavily dependent on time – as time increases, fluorescence intensity decreases (Fig, 13). The temperature of the laser itself also has a very high impact on fluorescence. Therefore, controlling for both the time dependency and for particle distribution heterogeneity is necessary before the true relationship between applied strain and induced fluorescence can be determined.

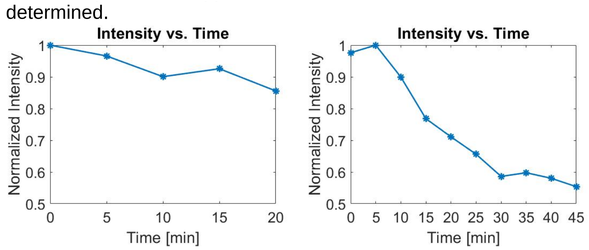

Fig. 13: Non-continuous use (left) vs continuous use (right) of laser

Conclusions

- A transport model for supercritical drying of silica aerogel was developed and solved to investigate the suction/spillage effects.
- Density and Sorét diffusion coefficient apparatus were designed and manufactured to measure the fluid properties.
- Drying shrinkage of silica gels was explicated by the need to maximize H-bonding interactions and the mass fractal structure of the framework.
- Fluorescence intensity of nanoparticles embedded aerogel monolith decreased with increasing applied load and time.